Journal of Hydrology 617 (2023) 128964

Contents lists available at ScienceDirect

Journal of Hydrology

journal homepage: www.elsevier.com/locate/jhydrol

Research papers

Quantitative partitioning of temporal origin of transpiration into pre- and post-plantation under deep-rooted vegetation on the Loess Plateau of China

Guangjie Chen [a,b,c], Wenjie Wu [a,b], Tingfang Meng [c,d], Mingyi Wen [a,b], Bingcheng Si [e], Jianqiang He [a,b], Min Li [a,b,*], Qin'ge Dong [a], Hao Feng [a,c,d,*], Kadambot H.M. Siddique [f]

[a] Key Laboratory of Agricultural Soil and Water Engineering in Arid and Semiarid Areas, Ministry of Education, Northwest A&F University, 712100 Yangling, Shaanxi Province, China
[b] College of Water Resources and Architectural Engineering, Northwest A&F University, 712100 Yangling, Shaanxi Province, China
[c] State Key Laboratory of Soil Erosion and Dryland Farming on the Loess Plateau, Institute of Soil and Water Conservation, Northwest A&F University, 712100 Yangling, Shaanxi Province, China
[d] State Key Laboratory of Soil Erosion and Dryland Farming on the Loess Plateau, Institute of Soil and Water Conservation, Chinese Academy of Sciences and Ministry of Water Resources, 712100 Yangling, Shaanxi Province, China
[e] Department of Soil Science, University of Saskatchewan, Saskatoon, SK S7N 5A8, Canada
[f] The UWA Institute of Agriculture and School of Agriculture and Environment, The University of Western Australia, Perth, WA 6001, Australia

ARTICLE INFO

This manuscript was handled by Marco Borga, Editor-in-Chief, with the assistance of Yuting Yang, Associate Editor

Keywords:
Water age
Transpiration
Deep-rooted vegetation
Loess Plateau

ABSTRACT

Deep-rooted vegetation transpires a considerable amount of deep soil water with different ages in the unsaturated zone. However, the tradeoffs between new water of transpiration (temporally originating from post-planting precipitation) and old water of transpiration (temporally originating from pre-planting precipitation) across the vegetation lifespan are poorly understood. In this study, we collected soil samples from beyond 28 m soil depth on the Loess Plateau of China to investigate the influence of deep-rooted vegetation on the age of soil water and analyze the proportion of new and old water of transpiration in the unsaturated zone under grassland, 22-year-old apple orchard, and 17-year-old peach orchard. Water isotopes (^{2}H, ^{18}O, and ^{3}H), solutes (chloride, nitrate, sulfate), and soil water content were used to identify the critical water ages in the unsaturated zone (one-year water age, water age corresponding to stand age, and the maximum water age of transpiration), and to determine soil water deficit, soil evaporation loss fraction, and potential groundwater recharge. The results showed that soil water mainly moved as piston flow in these soil profiles, and deep soil water largely came from heavy precipitation. Deep-rooted vegetation restrained new pore water velocity and potential groundwater recharge. New pore water velocity declined from 0.40 m yr^{-1} to 0.14 m yr^{-1} and 0.34 m yr^{-1} for apple and peach, respectively. Deep-rooted vegetation decreased groundwater recharge by 9.46 % for apple and 7.04 % for peach, compared to grassland. Over the vegetation lifespan, annual average transpiration was 500.56 mm yr^{-1} and 468.89 mm yr^{-1} with maximum water age of 63 years and 45 years for apple and peach, respectively. The transpiration of deep-rooted vegetation mainly used new water—94.97 % for apple and 97.47 % for peach. The total old water of transpiration was 553 mm for apple and 209 mm for peach. Our results identify the temporal sources of vegetation water use, offering new insights into the transpiration process of deep-rooted vegetation.

1. Introduction

Transpiration is the largest continental water flux returning to the atmosphere, representing about 80–90 % of terrestrial evapotranspiration (Good et al., 2015; Jasechko et al., 2013) and a dominant force in the global water cycle (Schlesinger and Jasechko, 2014). In the soil–plant–atmosphere continuum, vegetation on different land use types takes up water of different ages (Schenk and Jackson, 2005). Investigating the time of transpiration helps us understand water transit through the water cycle (Benettin et al., 2021). Thus, studies on transpiration water age are becoming increasingly valuable, especially under the situation of land use changes (Sprenger et al., 2018).

* Corresponding authors at: Key Laboratory of Agricultural Soil and Water Engineering in Arid and Semiarid Areas, Ministry of Education, Northwest A&F University, 712100 Yangling, Shaanxi Province, China.
E-mail addresses: limin2016@nwafu.edu.cn (M. Li), nercwsi@vip.sina.com (H. Feng).

https://doi.org/10.1016/j.jhydrol.2022.128964
Received 18 August 2022; Received in revised form 29 October 2022; Accepted 11 December 2022
Available online 15 December 2022

Transpiration water age of vegetation is a function of travel time from roots to the atmosphere, root access to water, and water held in the soil (Sprenger et al., 2019). Quantifying the water age of transpiration can help us to understand which water is used by vegetation (Allen et al., 2019). The absolute age of water taken up by vegetation varies from days to years, including precipitation water originating from previous growing seasons (Allen et al., 2019; Brinkmann et al., 2018) and stored soil water several decades old (Zhang et al., 2017). Overall, the water age transpired by vegetation largely depends on the different water ages available in the unsaturated zone (Sprenger et al., 2019).

In the unsaturated zone, multiple tracers are needed to identify water age since different tracers span different temporal scales (Abbott et al., 2016; Si and Jong, 2007). For example, natural variations in the stable isotopes of hydrogen and oxygen can be used to date water from precipitation events up to 3–5 years (Koeniger et al., 2016). Similarly, artificial chloride, nitrate, and sulfate can identify water age from the moment of fertilization. Tritium bulge has been used to chronicle water age in deep soils on the Loess Plateau in China (Li et al., 2018; Li and Si, 2018). Meanwhile, revealing the mechanism of soil water flow is necessary to interpret soil water age for tracers because it strongly depends on the flow mechanism. Under the assumption of piston flow, the inferred ages from historical tracers could be the actual soil water age (Bethke and Johnson, 2008). Therefore, multiple tracers can provide ideal signals of water age under piston flow mechanism in the unsaturated zone.

Depending on the climate and soil conditions, vegetation has different root distribution and root uptake strategies to access water of different ages. In arid and semiarid zones, vegetation develops deep roots that can access very old water (Beyer et al., 2016; Fan et al., 2017). The large consumption of old water in deep soil could break the connection between surface water and groundwater (Zhang et al., 2018). Once depleted, old soil water is difficult to recharge, due to correlation with deep soil water. Even, forming a dried soil layer where soil water was deficit (Jia et al., 2019). Several studies have focused on water deficit caused by excessive vegetation transpiration (Markewitz et al., 2010; Shao et al., 2021; Wang et al., 2011), investigating patterns of deep soil water depletion (Li et al., 2019b; Markewitz et al., 2010), spatial distribution and driving factors of water deficit (Liang et al., 2022; Wang et al., 2011) and eco-hydrological processes (Barua et al., 2021; Yang et al., 2022). Transpiration water age is useful for identifying which age of water is consumed. Recent studies found that deep-rooted vegetation transpired soil water older than the stand age (Li et al., 2018; Zhang et al., 2017). However, few studies have quantitatively explored the temporal origin of transpiration water for deep-rooted vegetation.

Due to excessive transpiration from deep soils, deep soil water deficit has been a major issue limiting water resource sustainability, which often occurs on the Loess Plateau in China (Huang and Shao, 2019; Jia et al., 2020, 2019; Wang et al., 2011). Zhang et al. (2017) reported that deep-rooted vegetation on the Loess Plateau transpired water up to several decades old. Considering the life cycle of perennial vegetation, soil water originating from pre-planting precipitation was called 'old water', while soil water from post-planting precipitation was called 'new water'. Old water consumption indicates the available precipitation resources cannot meet the vegetation transpiration during the growing period. Tradeoffs between the new and old water consumed throughout the vegetation life cycle become important for balancing deep soil water, but are rarely studied. Thus, this study aimed to distinguish the proportions of new and old water during the life-cycle transpiration of perennial deep-rooted vegetation (22-year-old apple orchard and 17-year-old peach orchard) on the Loess Plateau and to estimate the hydrological components affected by excessive transpiration. The objectives were to (1) determine the critical water ages and their corresponding depths in the unsaturated zone, (2) quantify new and old water in vegetation transpiration, and (3) evaluate the hydrological compartments of new and old water in vegetation transpiration.

2. Materials and methods

2.1. Study area

The study site was in the Tianhe Watershed (36°39′–36°40′ N, 109°22′–109°23′ E; Fig. 1a) in the central region of the Loess Plateau in China, the optimal area for the Grain for Green Project (Geng et al., 2020). The topography and landforms include ridges and gullies, with varying elevations of 988–1344 m. The soil layers are very thick, with groundwater table deeper than 100 m (Zhu et al., 2018). The deep loess profile comprises alternating glacial loess and interglacial paleosol. The soil texture is predominantly silty (silt content >60 %). The watershed is in a warm temperate semiarid zone with a continental monsoon climate. The long-term (1961–2018) average annual temperature is 10.1 °C, and the average annual precipitation is 543 ± 131 mm. About 70 % of average annual precipitation occur between June and September.

The study area has undergone dramatic land use changes since the implementation of the Grain for Green Project in 1999. Economic vegetation was expanded because orchards reduce soil water erosion and increase local farmer income. We chose a typical apple orchard converted from natural grassland in 1995, and a peach orchard converted from natural grassland in 2001, and nearby long-term natural grassland as the control treatment (Fig. 1b; Table 1).

2.2. Sampling and analyzing

Three soil cores were collected at the top platform of a hillside using a hollow-stem auger to 30 m depth for the apple orchard and grassland and 28 m for the peach orchard. Each core was separated into 20-cm intervals. Soil sampling was conducted on August 1st–6th in 2017 for the apple orchard and on August 1st–15th in 2018 for the peach orchard and the grassland. The soil samples were measured to determine soil water content, water isotopes, solute concentration (chloride, nitrate, and sulfate), and soil texture. Each soil sample was partitioned into three parts and placed into (1) an aluminum box for soil water content measurement through the oven-drying method (24 h at 105 °C); (2) a plastic bottle, sealed with sealing film, and stored at −18 °C for soil water extraction and subsequent stable isotopes and tritium measurements; (3) a fiber bag for measuring solute concentration and soil texture. Soil clay, silt, and sand fractions were measured using the pipette method (Gee and Bauder, 1986). For accurate estimations of the long-term soil evaporation loss fraction, soil samples to a depth of at least 10 m were extracted monthly to measure soil water content and stable isotopes from June to October 2018.

In addition, a hand auger with an inner diameter of 85 mm was used to sample roots between the diagonals of four similar-sized trees under the apple and peach orchards. Root samples were collected at 20-cm intervals to a depth of 3 m below the root zone. The samples were sieved through 1 mm mesh and washed with water. Then, the roots were collected with tweezers. Fine roots (≤2 mm) were analyzed with WinRHIZO imaging analysis software at 300 dpi (dots per inch). Fine root length density was calculated as the ratio of fine root length to soil volume.

A custom-made precipitation collector was placed in a bare area to collect incident precipitation (Fig. 1b). The collector comprised a funnel inserted and sealed into a cylindrical collection reservoir with a standard plastic ping-pong ball placed loosely over the opening of the funnel. Water filled the funnel during rain events, making the ping-pong ball float and allowing water to enter the reservoir. After the rain events, the ping-pong ball sat tight against the funnel opening, preventing debris from entering the reservoir and minimizing evaporation water loss. After removal from the collectors, the rainwater was stored at 4 °C before analysis. Precipitation samples were collected for each rain event between May 2018 and August 2020, totaling 123 samples.

The vacuum extraction method was used to extract water from the soil samples in the laboratory. The extraction efficiencies were 100 ± 2

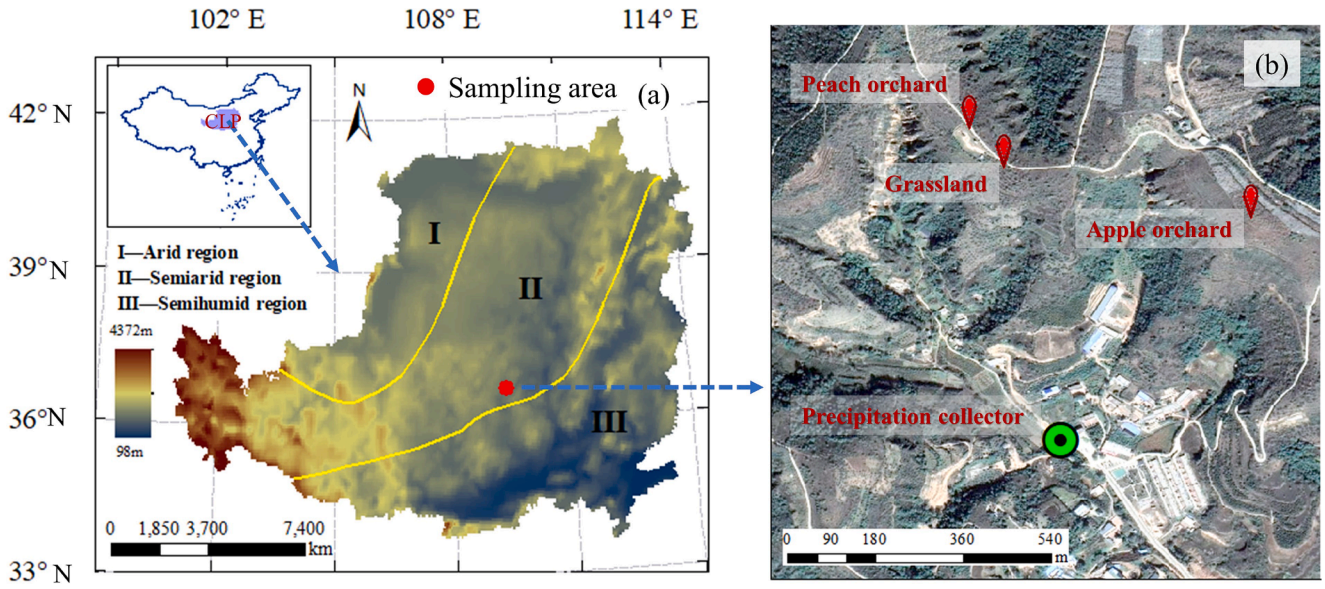

Fig. 1. (a) Location of the study area on the Loess Plateau of China, and (b) the sampling sites of the three land uses and precipitation collector in the study area.

Table 1
Characteristics of the apple orchard, peach orchard, and grassland investigated.

Species	Stand age (year)	Height (m)	DBH (cm)	Density (m)	Elevation (m)	Soil texture (%)		
						Clay	Silt	Sand
Apple	22	3.20 (0.15)	16.53 (0.85)	3.5 × 3.0	1285	12.68 (0.04)	66.58 (0.09)	20.74 (0.09)
Peach	17	1.60 (0.12)	18.46 (1.54)	3.0 × 3.0	1228	12.46 (0.03)	68.40 (0.05)	19.14 (0.05)
Grassland	–	–	–	–	1224	12.84 (0.04)	65.01 (0.06)	22.15 (0.07)

Note: DBH: diameter at breast height; Numbers in brackets are standard deviations.

%. Pure soil water (8 mL) was mixed with 12 mL scintillation solution (Hisafe3) in a 25 mL standard plastic bottle. After 24 h of dark adaptation, the tritium count was recorded using a low-background liquid scintillation counter (Quantulus 1220, PerkinElmer, Singapore). The results were expressed in TU units with a detection limit of 10.5 TU, defined as 3.29 times the standard deviation of the measurement according to Armbruster and Pry (2008). The δ^2H and $\delta^{18}O$ compositions in soil water were determined with a liquid water isotope analyzer (IWA-45EP, Los Gatos Research, USA) with a measurement accuracy of ±1.5 ‰ for δ^2H and ±0.2 ‰ for $\delta^{18}O$. The isotopic composition of each water sample was expressed as:

$$\delta X = \left(\frac{R_{sample}}{R_{standard}} - 1\right) \times 1000‰ \quad (1)$$

where X is ^2H or ^{18}O; R_{sample} and $R_{standard}$ are the ratios of $^2H/^1H$ or $^{18}O/^{16}O$ in the sample and the standard (Vienna Standard Mean Ocean Water), respectively.

Deionized water (25 mL) was added to 5 g oven-dried soil samples to determine chloride, nitrate, and sulfate concentrations in soil water. The samples were then agitated on a reciprocal shaker table for 1 h and centrifuged at 5000 rpm for 30 min. The concentration of the supernatant solution was analyzed by ion chromatography (Dionex ICS-1100, Thermo Fisher Scientific, USA) and then converted to pore water chloride, nitrate, and sulfate concentrations.

2.3. Partitioning the temporal origins of transpiration water into pre- and post-plantation

In perennial deep-rooted vegetation, the water age of transpiration was reflected by resolving the temporal origin of soil water, ignoring the time of transpiration from soil to xylem. The water age of transpiration of deep-rooted vegetation was divided into two parts according to its temporal origin: the post-planting new water and pre-planting old water. Soild fertilizers, containing large amounts of chloride, nitrate, and sulfate, were applied at planting. Thus, the water age of the deepest soil solute peak was considered the moment at planting. With this soil depth as the critical layer between old and new water, the whole profile was partitioned into two sub-profiles (Fig. 2). No exchange of soil water occurred at the interface between new and old water if piston flow dominated soil water recharge. We established the water balance equations for each of the two sub-profiles according to the fate of the soil water.

In the new water zone, transpiration was derived as the difference between the net precipitation and soil evaporation loss and the soil water recharge during vegetation planting (Fig. 2b). In the old water zone, transpiration came from the deep soil water deficit, soil water recharge, and loss of groundwater recharge under deep-rooted vegetation (Fig. 2c). The cumulative chloride age in the unsaturated zone was calculated to determine the maximum water age of transpiration, which did not need a steady state (Huang et al., 2020). However, chloride input from fertilization was not available for this study. Fortunately, the tritium peak could be used to trace the soil water age in 1963 (Li et al., 2018; Li and Si, 2018). The maximum water age of transpiration was determined using a method that combined the tritium peak with the chloride cumulative age. More specifically, if the maximum water consumption depth exceeded the tritium peak depth, the maximum water age of transpiration was considered the sum of the water age of tritium peak and the cumulative chloride age below the tritium peak. When the depth of maximum water consumption was shallower than the tritium peak, the maximum water age of transpiration was calculated as the difference between the water age at the tritium peak and the chloride

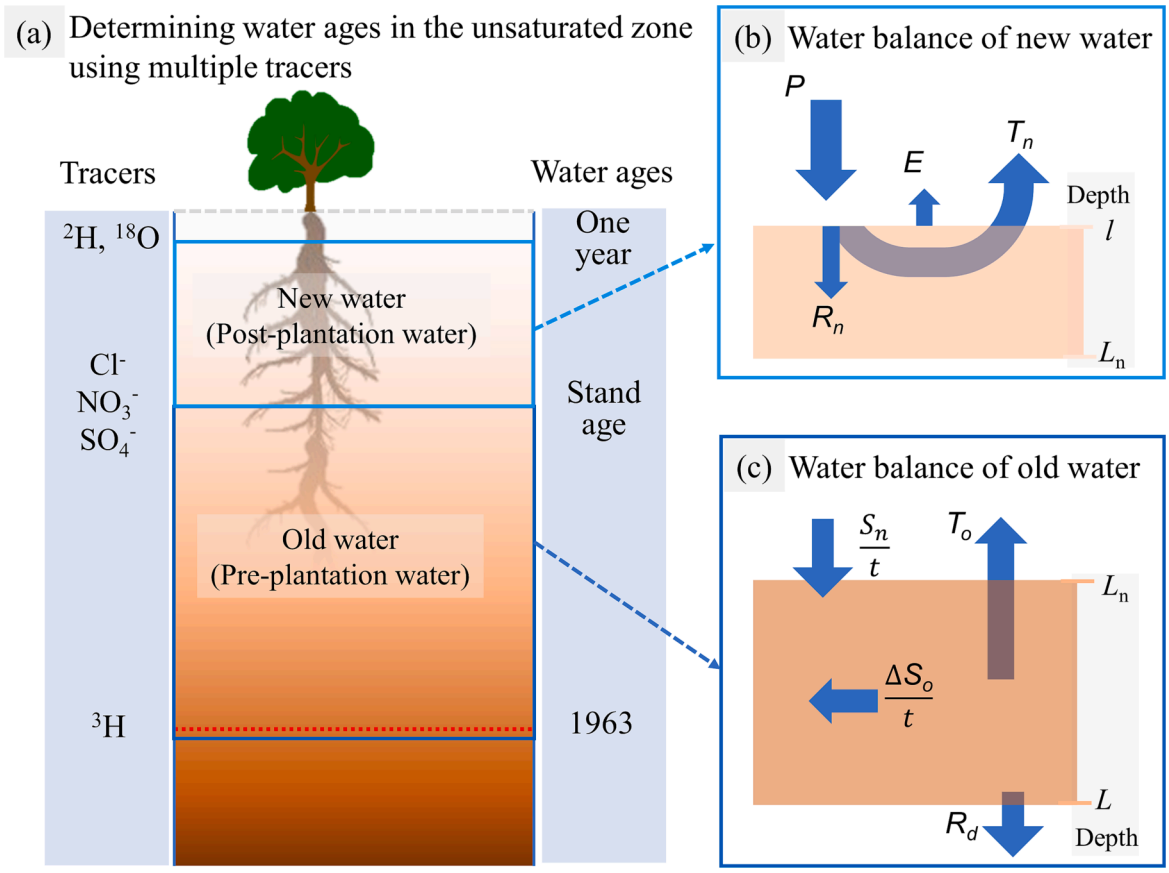

Fig. 2. Conceptual model of water ages and water balance of new and old water in the unsaturated zone. (a) Definition of main three soil water ages in the unsaturated zone. Soil water age at given soil depth and seasonal variations of stable isotopes (^2H, ^{18}O) indicates the current year of water. Soil water age at the lowermost peak depths of chloride, nitrate, and sulfate indicates the planting year. Soil water age at the depth of tritium peak indicates the year of 1963. (b) Hydrological compartments of new water. When precipitation fell on soil surface, some precipitation water was directly evaporated into the atmosphere as water vapor, some was transpired through root water uptake, and the remainder was recharged into deep soil layer. The symbols of P, E, T_n, and R_n refer to precipitation, evaporation, new water transpiration, and soil water recharge; l and L_n refer to the depth of soil water active layer and interface between new and old water, respectively. (c) Hydrological compartments of old water. Root water uptake from deep soil profile caused deep soil water deficit and reduced groundwater recharge. The symbols of ΔS_o, t, T_o, $\frac{S_n}{t}$, and R_d refer to soil water deficit, stand age, old water transpiration, soil water recharge, and groundwater recharge under deep-rooted vegetation; L_n and L refer to the depth of the interface between new water and old water and the maximum water consumption, respectively.

cumulative age at depth from root depth to tritium peak (Fig. 2). The following sections elaborate on the hydrological components for partitioning the temporal origins of transpiration water into pre- and post-plantation (Fig. 3).

2.3.1. Soil water deficit

Soil water in the deep soil profile under shallow-rooted grassland was considered the initial soil water status under deep-rooted vegetation (Zhang et al., 2018). Soil water deficit was the difference between soil water storage under grassland and deep-rooted vegetation. Soil water deficit was calculated(Eqs. (2)–(4)), ignoring change in soil water content in the active layer.

$$\Delta S_a = \sum_{l}^{L} (\theta_s - \theta_d) \tag{2}$$

$$\Delta S_n = \sum_{l}^{L_n} (\theta_s - \theta_d) \tag{3}$$

$$\Delta S_o = \sum_{L_n}^{L} (\theta_s - \theta_d) \tag{4}$$

where ΔS_a, ΔS_n, and ΔS_o are the total soil water deficit, soil water deficit of new water, and soil water deficit of old water (mm); $\theta_s(z)$ and $\theta_d(z)$ are the volumetric soil water contents of shallow-rooted and deep-rooted vegetation (cm^3 cm^{-3}), respectively; L is the maximum depth of water consumption (mm);l is depth of the soil water active layer (mm); L_n is the interface depth between old and new water, the depth of the deepest solute peak in the soil (mm).

2.3.2. Soil water recharge for new water

The pore water velocity of the new water is defined as the depth of the new water divided by the corresponding time (Eq. (5)). The new water recharge is defined as the new water storage divided by the corresponding water age (Eq. (6)).

$$v_n = \frac{L_n}{t} \tag{5}$$

$$R_n = \frac{S_n - \Delta S_n}{t} = \frac{\sum_{l}^{L_n} \theta_d}{t} \tag{6}$$

where v_n is new pore water velocity; R_n is new water recharge; S_n is soil water storage relative to grassland; ΔS_n is soil water deficit of new water; t is the stand age of deep-rooted vegetation.

2.3.3. Evapotranspiration from new water

When planting deep-rooted vegetation, some precipitation returned to the atmosphere through soil evaporation and plant transpiration,

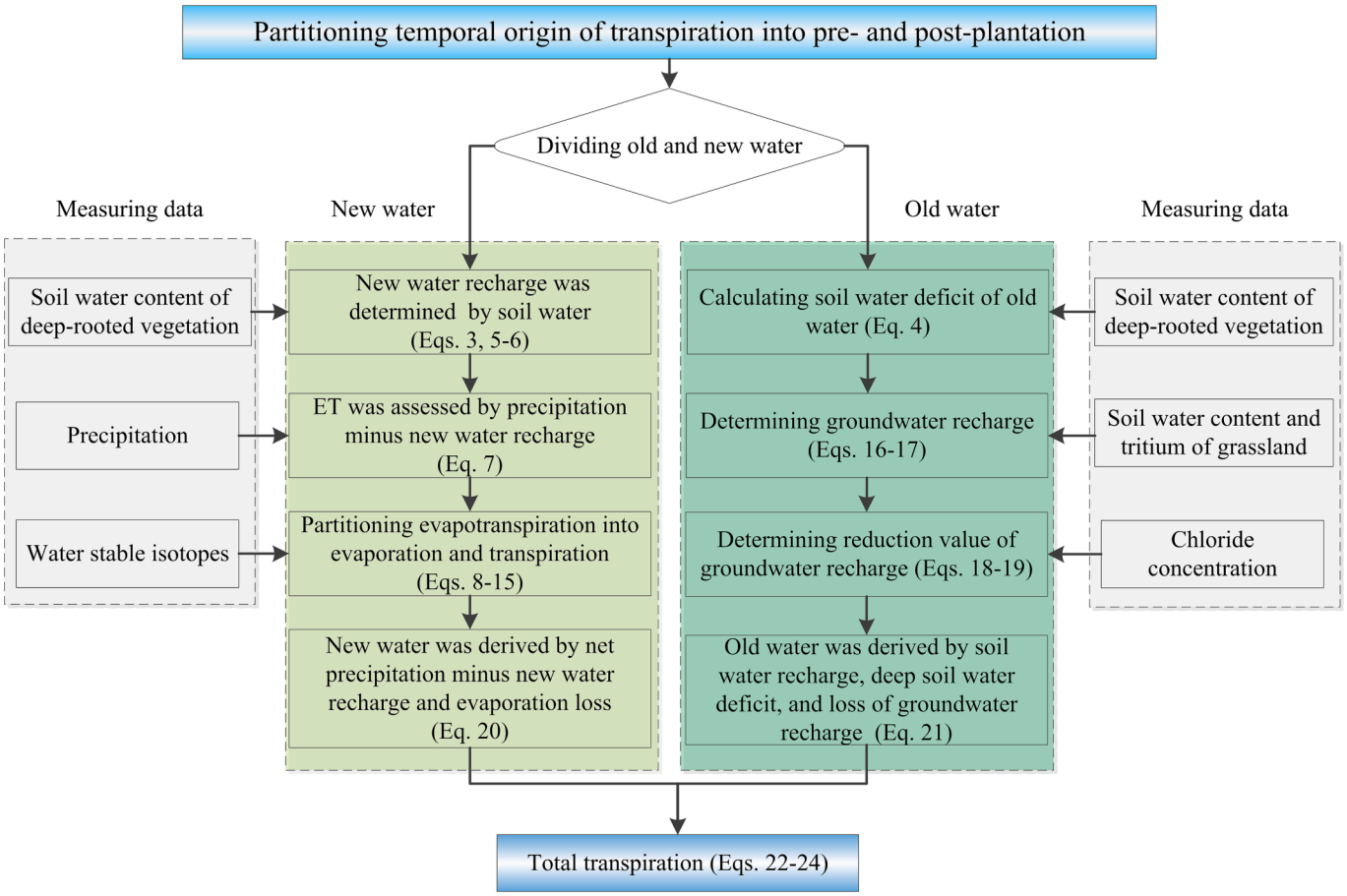

Fig. 3. Flowchart of the equations used in the methodology of water balance based on water ages in the unsaturated zone.

while the remainder was recharged into the soil. Hence, the evapotranspiration from new water during this time was equivalent to the precipitation minus the new water recharge (Eq. (7)).

$$ET_n = P - R_n \tag{7}$$

where ET_n is the evapotranspiration from new water (mm yr^{-1}), and P is annual average precipitation during vegetation planting (mm yr^{-1}).

2.3.4. Soil evaporation loss fraction

Soil evaporation and plant transpiration had different temporal attributes in the long-term water balance under deep-rooted vegetation. Soil evaporation loss, which took place in topsoil, was considered part of new water. Evapotranspiration partitioning was adopted to compare old water of transpiration with new water of transpiration. We used the model of steady-state isotope mass balance (Eq. (8)) to calculate the fractions of evaporation loss. This model was derived from the evapotranspiration partitioning approach (Kool et al., 2014) and then reframed to estimate evaporation loss (Al-Oqaili et al., 2020). It assumed input water was balanced by fractionated water (evaporation) and non-fractionated water (transpiration and groundwater recharge). Soil evaporation (E) can be calculated as the product of evaporation loss fraction and precipitation. The average value of soil water evaporation fraction (f) can be estimated (Eqs. (8) and (9)).

$$f = \frac{E}{P} = \frac{\delta_p - \delta_s}{\delta_E - \delta_s} \tag{8}$$

$$\delta_I = f \times (\delta_E - \delta_s) + \delta_s \tag{9}$$

The input water δ_p (‰) originated from local precipitation (without irrigation). Thus, the lc-excess value of the effective input water lc_I (Eq. (10)) was calculated based on Eq. (9) and the dual-isotope method (Xiang et al., 2021).

$$lc_I = [f \times (\delta_E - \delta_s) + \delta_s]_{2_H} - a[f \times (\delta_E - \delta_s) + \delta_s]_{18_O} - b \tag{10}$$

where lc_I is the lc-excess value of the effective input water (‰), set to zero because precipitation is the only soil water source, and δ_s is the soil water isotope (‰). The soil water isotopes below the soil water active layer were used for the grassland, while the soil water isotopes between l and L_n depths were used for the deep-rooted vegetation. δ_E is the isotopic composition of evaporated water (‰) (Eq. (11)) based on the Craig-Gordon model (Craig and Gordon, 1965).

$$\delta_E = \frac{(\delta_S - \varepsilon^+)/\alpha^+ - h\delta_A - \varepsilon_K}{1 - h + \varepsilon_K/1000} \tag{11}$$

where ε^+ (‰) and α^+ (–) are the kinetic fractionation factor, $\varepsilon^+ = (\alpha^+ - 1) \times 10^3$; δ_A is the isotopic composition of atmospheric water vapor (‰), estimated as $\delta_A = (\delta_p - \varepsilon^+)/\alpha^+$; and α^+ is a function of temperature (Eqs. (12) and (13)) (Gibson et al., 2008; Horita and Wesolowski, 1994). For the methods and uncertainty of estimating δ_A, please refer to Skrzypek et al. (2015). ε_k was calculated from Eqs. ((14) and (15)).

$$10^3 ln\left[\alpha^+(^2H)\right] = \frac{1158.8T^3}{10^9} - \frac{1620.1T^2}{10^6} + \frac{794.84T}{10^3} - 161.04 + \frac{2.9992 \times 10^9}{T^3} \tag{12}$$

$$10^3 ln\left[\alpha^+(^2o)\right] = 7.685 + 6.7123\frac{10^3}{T} - 1.6664\frac{10^6}{T^2} + 0.3504\frac{10^9}{T^3} \tag{13}$$

$$\varepsilon_k(^2H) = n(1-h)(1-0.9755) \tag{14}$$

$$\varepsilon_k(^{18}o) = n(1-h)(1-0.9723) \quad (15)$$

where parameter n is the aerodynamic diffusion ranging from 0.5 (saturated soil conditions) to 1.0 (very dry soil conditions). The value of n was set as 0.75 because the evaporating soil layer had alternate saturating and drying conditions over time in this study. We estimated the values of α^+ and ε_k based on long-term (1961–2018) average daily temperature and relative humidity.

2.3.5. Groundwater recharge and pore water velocity

For the shallow-rooted zone, long-term annual groundwater recharge was determined using the tritium peak method (Eqs. (16) and (17)) (Allison et al., 1990).

$$R_s = \frac{\sum_l^{L_t}\theta_s}{t-1} = v\bar{\theta}_s \quad (16)$$

$$v = \frac{L_t - l}{t-1} \quad (17)$$

where R_s is groundwater under the grassland (mm yr^{-1}); L_t is tritium peak depth (mm); t_t is the time between the sampling year and 1963 (yr); and v is pore water velocity under the grassland (mm yr^{-1}). These two equations, assumed that soil water from precipitation took one year to penetrate the soil water active layer.

Groundwater recharge for deep-rooted vegetation was determined as the difference between potential groundwater recharge under grassland and the loss of soil water recharge under deep-rooted vegetation (Eq. (18)).

$$R_d = R_s - \frac{\sum_L^{L_s}\theta_s}{t} \quad (18)$$

where R_d is potential groundwater recharge under deep-rooted vegetation (mm yr^{-1}); depth (L) corresponding to water age is t_r, which can be calculated using the chloride cumulative age method (Huang et al., 2020); L_s is the soil depth corresponding to water age t_r under grassland.

The pore water velocity in the entire root zone was estimated as the ratio between the maximum water consumption depth and the corresponding water age (Eq. (19)).

$$v_r = \frac{L}{t_r} \quad (19)$$

where v_r is the pore water velocity in the entire root zone (m yr^{-1}); L is the maximum depth of water consumption (m); t_r is the water age corresponding to the maximum root depth (year).

2.3.6. Transpiration from new water and old water

For new water, precipitation was divided into evaporation, transpiration, and soil water recharge. Thus, transpiration from new water can be calculated (Eq. (20)). Old water of transpiration originated from soil water deficit, soil water recharge, and groundwater recharge (Eq. (21)). Total transpiration was equal to the sum of new water and old water transpiration (Eq. (22)).

$$T_n = P - E - R_n \quad (20)$$

$$T_o = \frac{\Delta S_o}{t} + \frac{S_n}{t} - R_d \quad (21)$$

$$T_a = T_n + T_o \quad (22)$$

For the entire deep profile (Fig. 2a), total transpiration was calculated with Eq. (23). The actual annual evapotranspiration (Eq. (24)) was equal to the sum of transpiration (Eq. (22) or (23)) plus evaporation:

$$T_a = P + \frac{\Delta S_a}{t} - R_d - E \quad (23)$$

$$ET = T_a + E = P + \frac{\Delta S_a}{t} - R_d \quad (24)$$

2.4. Statistical analysis

The difference between the means of the two treatments can be tested using the student's t-test:

$$t = \frac{\bar{x} - \bar{y}}{\sqrt{\sigma_x^2 + \sigma_y^2}} \quad (25)$$

where $\bar{x}$ and $\bar{y}$ are the means and σ_x and σ_y are the standard errors of variables x and y, respectively. A significant difference is considered when the value is greater than 1.96 (P = 0.05).

3. Results

3.1. Water isotopes in precipitation and soil water

Monthly $\delta^{18}O$ values in precipitation ranged from −13.8 to −3.2 ‰ with a volume-weighted mean value of −9.1 ± 1.0 ‰ (mean ± SD). Monthly δ^2H values ranged from −95.6 to −14.3 ‰ with a volume-weighted mean value of −63.1 ± 7.0 ‰ (Fig. 4).

Soil water isotopes were located close to but below LMWL (Fig. 4), revealing that soil water came from precipitation. Soil water isotope values were close to the monthly volume-weighted isotope values of large precipitation amounts (July–September). Average deep soil water isotopes were close to isotope signals from most heavy precipitation (Fig. S1), indicating that deep soil water was mainly from heavy precipitation. Soil water isotopes were more enriched than volume-weighted precipitation values, and the slopes and intercepts were lower than those of LMWL. The slopes of the evaporation line of soil water isotopes were similar: 5.82 ± 0.74 for grassland, 5.75 ± 0.47 for apple orchard, and 5.53 ± 0.35 for peach orchard. Meanwhile, the fitted tritium profiles had bell-shaped distributions within each soil profile (Fig. 5d), showing that the piston flow dominated the recharge mechanism.

3.2. Water ages of soil profiles

Soil water and soil water isotopes in the 0–2 m soil layer fluctuated

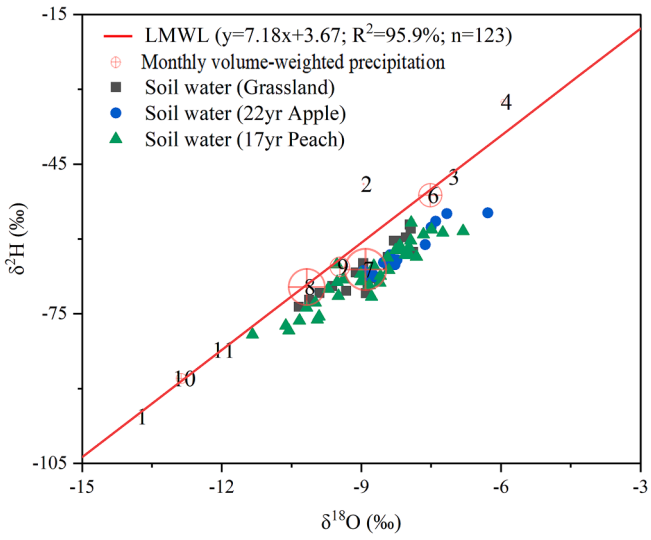

Fig. 4. Dual isotopes plot of precipitation, and soil water under different land use types. The numbers represent 11 months (no recorded precipitation in December during the sampling period), and red circle size denotes monthly mean precipitation.

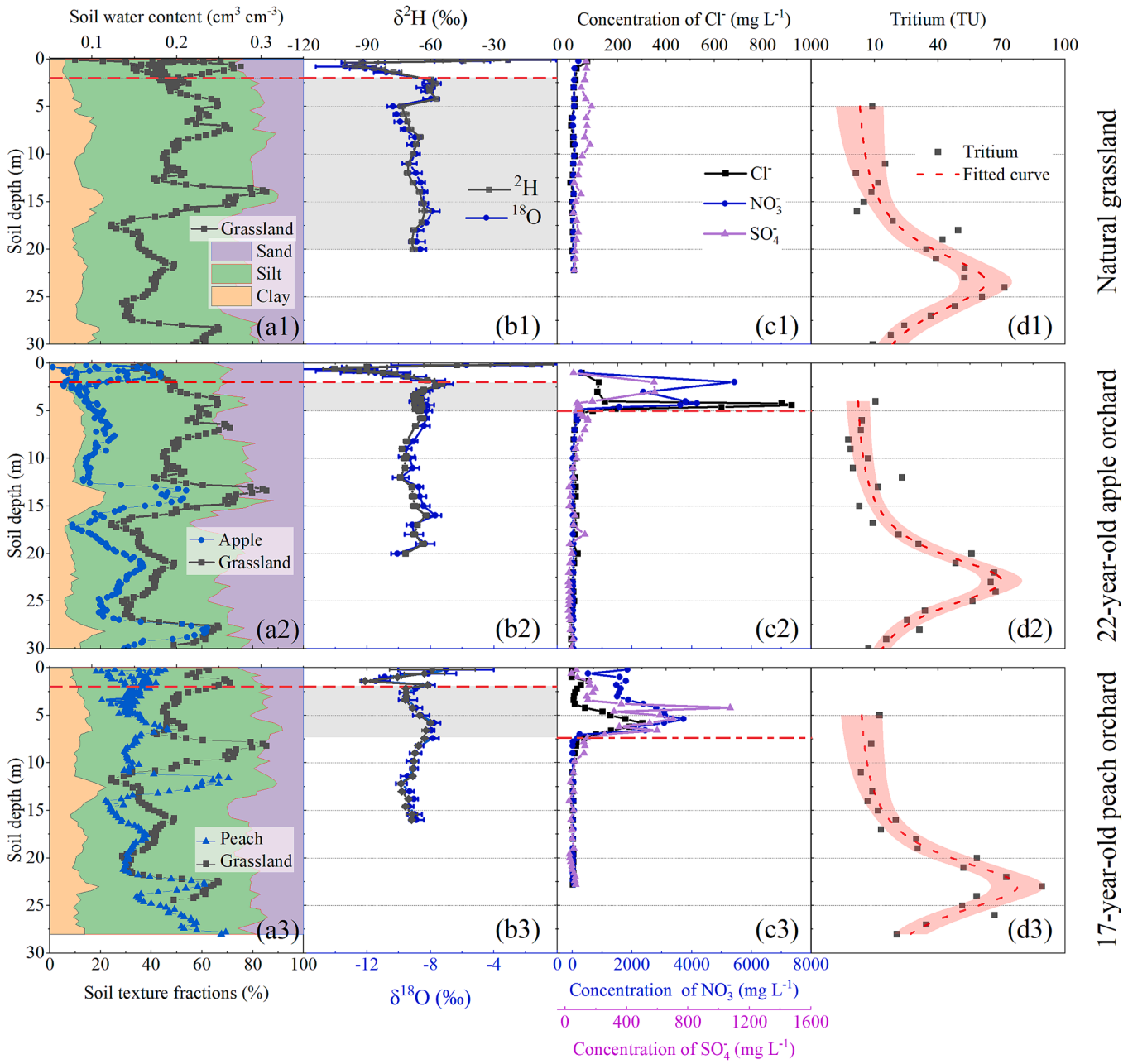

Fig. 5. Soil profiles for (a) soil water, (b) ^{2}H and ^{18}O, (c) solute, and (d) tritium under natural grassland, 22-year-old apple orchard, and 17-year-old peach orchard (denoted by 1, 2, and 3, respectively). The dotted lines (in a) represent the depth of soil water active layer. Error bars (in b) are standard errors of the means (N = 5). Data from the gray areas were used to calculate the fraction of soil evaporation loss. The dotted lines (in c) represent the maximum depth of new water. The dotted lines and light red areas (in d) were fitted tritium profiles using the Lorentz function, and fitted 95 % confidence intervals, respectively.

greatly under the three vegetation types due to alternating dry and wet periods caused by precipitation and evapotranspiration within the year (Fig. 5a, b), indicating the three land uses have the same depths of soil water active layer. So, the water age of soil water within 2 m soil depth was determined as one year. Ignoring soil water storage in soil water active layer, soil water deficit was 1819 mm (to 26.4 m) under the apple orchard and 589 mm (to 19.6 m) under the peach orchard (Fig. 5a).

Chloride, nitrate, and sulfate concentrations did not change dramatically in the deep soil profile under grassland (Fig. 5c1), but noteworthy peaks occurred at 5 m under the apple orchard and 7.4 m under the peach orchard, caused by historical fertilization (Fig. 5c2, c3). The solutes below the interface layer were not affected by fertilization and did not change sharply with depth. Thus, soil depths of about 5 m and 7.4 m were considered the critical interface layer for new and old water under the apple and peach orchards, respectively. The average velocity of new pore water was about 0.14 m yr^{-1} under the apple orchard and 0.34 m yr^{-1} under the peach orchard.

The fitted tritium profiles had bell-shaped distributions within the soil profile (Fig. 5d). Peak concentrations occurred at 23.43 ± 0.38 m under the grassland, 22.88 ± 0.10 m under the apple orchard, and 22.95 ± 0.29 m under the peach orchard. Statistically significant differences in peak depths occurred between the deep-rooted orchards and grassland ($P < 0.05$). According to the fine root length density (FRLD) from the soil surface to the maximum rooting depth of the two tree species (Fig. 6), the maximum rooting depths under the apple orchard and the peach orchard were the same as the maximum water consumption depths (26.4 and 19.6 m, respectively). Based on the tritium peak depth and chloride accumulative age method, the maximum water age of transpiration was

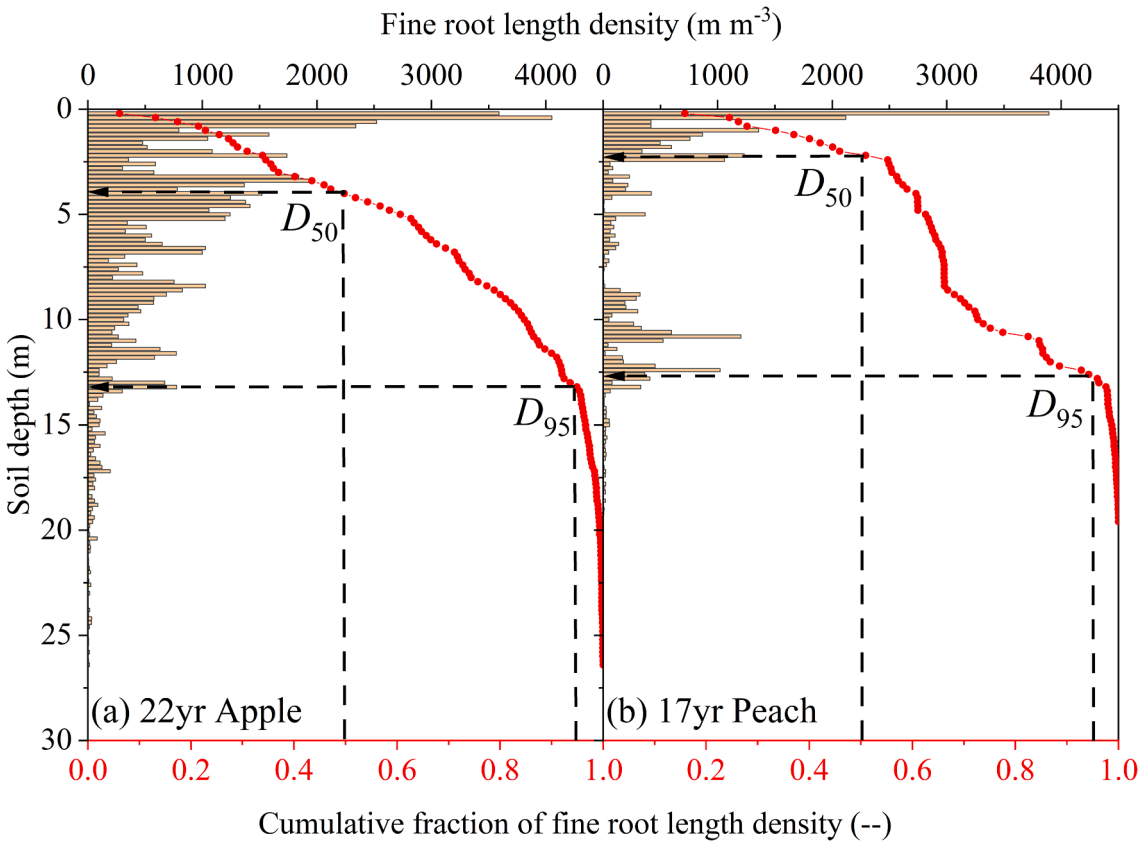

Fig. 6. Fine root length density and cumulative fine root length density of 22-year-old apple trees (a) and 17-year-old peach trees (b). The symbols of D_{50} and D_{95} represent the soil depth reached by 50 % and 95 % of the total roots, respectively.

about 63 years under the apple orchard and 45 years under the peach orchard. The average pore water velocities through the entire root zone were about 0.40, 0.39, and 0.40 m yr^{-1} for grassland, apple orchard, and peach orchard, respectively.

3.3. Partitioning temporal origins of transpiration

3.3.1. New water of transpiration

The grassland had 76.82 mm yr^{-1} of groundwater recharge (Eq. (16); Table 2) and 5.65 % soil evaporation loss fraction (Eq. (8)), such that the average annual transpiration under grassland was 436.13 mm yr^{-1}. The apple orchard had 265.02 mm soil water storage derived from new water (2–5 m depth), 508.99 mm yr^{-1} average evapotranspiration for a water age of 22 years, 6.74 % soil evaporation loss fraction (Eq. (8)), and thus about 475.39 mm yr^{-1} average new water of transpiration. The peach orchard had about 559.82 mm yr^{-1} precipitation input since the planation year. Soil water deficit of new water (2–7.4 m) was about 834.35 mm, with about 510.74 mm yr^{-1} average annual evapotranspiration for water age of 17 years and 7.14 % soil evaporation loss fraction. Consequently, the peach orchard had about 473.23 mm yr^{-1} average new water of transpiration.

3.3.2. Old water of transpiration

Under the apple orchard, the average groundwater recharge declined to 69.55 mm yr^{-1} (Eq. (18)). Average annual soil water deficit with water age >22 years was about 65.48 mm yr^{-1} for the apple orchard, while soil water recharge was 29.24 mm yr^{-1}. Based on Eq. (21), old water of transpiration was 25.17 mm yr^{-1}. Under the peach orchard, the average groundwater recharge was 71.41 mm yr^{-1}. Soil water consumption from old water was about 360.82 mm, and soil water recharge was 62.48 mm yr^{-1}. Hence, old water of transpiration was about 12.29 mm yr^{-1}.

4. Discussion

4.1. Soil water age signals in the unsaturated zone

Soil water age is zero when precipitation falls on the soil surface

Table 2
Estimated hydrological components of new and old water balance in the 22-year-old apple orchard, the 17-year-old peach orchard, and grassland.

	22-year-old apple orchard		17-year-old peach orchard		Grassland
Water age (yr)	0–22 (new water)	>22 (old water)	0–17 (new water)	>17 (old water)	–
Precipitation (mm yr^{-1})	521.04	–	559.85	–	538.94
Evaporation (mm yr^{-1})	33.60	–	37.51	–	25.99
Groundwater recharge (mmyr^{-1})	–	69.55	–	71.41	76.82
Soil water recharge (mm yr^{-1})	12.05	29.24	49.08	62.48	–
Soil water deficit (mm yr^{-1})	17.19	65.48	13.40	21.22	–
Transpiration (mm yr^{-1})	475.39	25.17	473.23	12.29	436.13
Total transpiration (mm yr^{-1})	500.56		485.52		436.13

Note: Precipitation values are average annual values in 1995–2017 for the apple orchard, in 2001–2018 for the peach orchard, and 1963–2018 for grassland.

(Sprenger et al., 2019, 2018). At our experimental site, snowmelt is relatively small with an average annual value of 18.4 mm, causing a slight infiltration delay of a few days. However, this lag time can be ignored in this study's annual-scale. As a result, we assumed that precipitation time is consistent with soil water infiltration time.

The measured tritium profiles showed that the historical rainwater tracer signal over time in the unsaturated soil profile (Fig. 5d). The bell-shaped tritium distribution indicated that soil piston flow dominated in the non-fractured unsaturated zone (Li and Si, 2018; Lin and Wei, 2006). Post-bomb tritiated rainwater diffused into the soil matrix, resulting in a bell-shaped tritium distribution within the soil profile, resembling soil piston flow (Foster, 1975), consistent with stable isotopes at other sites on the Loess Plateau of China (Yang and Fu, 2017). The estimated old and new water failed to mix via piston flow. To our knowledge, preferential flow only occurs in some restricted low-lying areas on the Loess Plateau (Huang et al., 2019; Xiang et al., 2019). Our study site is located on the top platform of a hillside, where it is unlikely that preferential flow will occur. Thus, age-dating tracers measured the actual water age in our study.

We determined three critical water ages in the unsaturated zone using multiple tracers and soil water content measurements: one-year water age, water age corresponding to stand age, and the maximum water age of transpiration. The soil water active layer was defined as 0–2 m after measuring soil water dynamics and variation of stable isotopes in the unsaturated zone over one year (Fig. 5a, b), consistent with Wu et al. (2021). The soil water active layer is usually considered for one year's water (Tao et al., 2021), undergoing multiple soil water depletion and recharge process throughout the year. So, one-year-old water in the unsaturated zone will not affect the water cycle in the long term (Suo et al., 2018). Water age corresponding to stand age was determined by artificially-adding solutes to a depth that reflects the effect of deep-rooted vegetation on the new water recharge rate. The depth of 22-year water age was 5 m with a new water recharge rate of 0.14 m yr^{-1} under the apple orchard while the depth of 17-year water age was 7.4 m with a new water recharge rate of 0.34 m yr^{-1} under the peach orchard, showing that vegetation type affects the depth of water year corresponding to stand age. As used in previous studies, the maximum transpired water age was determined using tritium peaks combined with the chloride accumulative age method (Huang et al., 2018; Lu et al., 2020). Our study found that the 22-year-old apple orchard transpired water above the 26.4 m soil layer with a maximum water age of 63 years, while the 17-year-old peach orchard transpired water above the 19.6 m soil layer with a maximum water age of 45 years, indicating deep-rooted vegetation transpired soil water that was older than the stand age.

4.2. Partitioning temporal origin of transpiration into pre- and post-plantation

Our results showed that deep-rooted vegetation transpired water mainly from new water (Table 2). The new water located in shallow soil was easily accessible to vegetation roots (Fan et al., 2017). Meanwhile, more than half of FRLD (61 % for apple and 66 % for peach) was concentrated in new water (Fig. 6), indicating dense root networks in shallow soil more likely to take up new water than old water. In addition, new water came from annual precipitation, while old water came from the soil water formed by pre-planting precipitation. The long-term average new water source was 543 mm yr^{-1}, while the old water source was 76.82 mm yr^{-1} under the grassland. Furthermore, deep-rooted vegetation uses new water in the early stages of planting with its shallow root system and low transpiration requirements (Zhang et al., 2020). The proportion of old water of transpiration to total transpiration was small (5.03 % for apple, and 2.53 % for peach). However, the accumulative amount of transpired old water was not negligible after the land use change, reaching 553 mm for apple orchard and 209 mm for the peach orchard, since it is not available for precipitation recharge after land use changes. Total old water consumption was 7.2 times higher for the apple and 2.7 times higher for the peach than annual average groundwater recharge under grassland.

Old water of transpiration was 25 mm yr^{-1} for the apple orchard and 12 mm yr^{-1} for the peach orchard, indicating that the 22-year-old apple trees used more old water for transpiration than the 17-year-old peach trees, which was likely due to (1) deeper rooting depth of apple trees (26.4 m vs. 19.6 m); (2) different root water uptake strategies. For example, Wu et al. (2022) found that peach trees used more shallow soil water, representing new water, than apple trees; (3) slightly older stand age.

4.3. Hydrological compartments of new and old water

This study decomposed the soil water balance method by combining soil water, water isotopes, and chloride concentrations. The ET values in this study accounted for 102.52 % of the average annual precipitation under the apple orchard, 93.43 % under the peach orchard, and 80.92 % under the grassland, within the range (82–110 %) reported on the Loess Plateau (Li et al., 2019a). The estimated soil evaporation loss fraction (f = E/P) values were about 6.58 % for the apple orchard, 7.14 % for the peach orchard, and 4.84 % for the grassland, close to the lower limit (5–15 %) reported by Xiang et al. (2021) using the same method on the Loess Plateau. Groundwater recharge declined by 9.46 % for the apple orchard and 7.04 % for the peach orchard after land use conversion relative to the grassland, similar to the 6.1 % reduction for alfalfa plantation and 11.0 % reduction in the unsaturated zone (Li et al., 2014; Turkeltaub et al., 2018).

The conversion of natural grassland into deep-rooted vegetation led to a series of hydrological changes, with new pore water velocity declining from 0.40 m yr^{-1} to 0.14 m yr^{-1} and 0.34 m yr^{-1} for apple and peach, respectively, indicating that deep-rooted vegetation decreased recharge rate of new water. Annual precipitation recharges to the maximum depth of 2 m (Fig. 5a), leading to water deficits when new water below 2 m is consumed in the rooting zone. Therefore, deep-rooted vegetation had greater new water of transpiration than grassland. Old water of transpiration largely led to a serious old water deficit, with a small effect on groundwater recharge. Old water of transpiration by the apple orchard resulted in old water deficit, equivalent to 85 % of annual average groundwater recharge under grassland (Table 2). Groundwater recharge was only reduced by 9.5 % under the apple orchard and 7.0 % under the peach orchard compared to grassland due to a lagged response in the unsaturated zone (Li et al., 2019c; Rossman et al., 2014). The phenomenon of delayed tracer breakthrough in groundwater recharge was demonstrated in a lysimeter experiment (Benettin et al., 2021).

4.4. Uncertainty of this study

The uncertainty of this study comes largely from the (1) soil evaporation loss fraction due to the short-term observation of water isotopes in precipitation; (2) potential groundwater recharge for deep-rooted vegetation due to the uncertainty of chloride inputs. The volume-weighted average water isotopes used in this study were -9.1 ± 1.0 ‰ for $\delta^{18}O$ and -63.1 ± 7.0 ‰ for $\delta^{2}H$, depleted than the values reported in the mid-1980s to 1990s (-8.1 ± 3.7 ‰ for $\delta^{18}O$ and -58.2 ± 27.4 ‰ for $\delta^{2}H$) (Liu et al., 2014). Given the earlier precipitation isotopes were used, the estimated soil evaporation loss fraction had similar results to our study (5.7 % vs. 5.6 % for grassland, 6.5 % vs. 6.7 % for the apple and 6.9 % vs. 7.1 % for the peach). For the uncertainty of chloride input, we calculated an annual chloride concentration of 1.32 mg L^{-1} based on the tritium profile under grassland, which was close to other studies in the surrounding areas: 1.4 mg L^{-1} (Gates et al., 2011), 1.0 mg L^{-1} (Li et al., 2017) and 0.8 mg L^{-1} (Huang et al., 2018).

To identify land use impacts, we selected grassland adjacent to deep-rooted vegetation (distance <500 m) to ensure the same climatic and

hydrological conditions. Further, the spatial variations in soil profiles can be excluded due to the similar soil water distribution and soil texture fractions (Fig. 5a). In addition, seasonal variations in soil water and water isotopes were above 2 m (Fig. 5a, b), so the sampling season did not impact the changes in water isotopes, chloride, and soil water below 2 m soil layers. Therefore, our sampling process is reliable for data acquisition.

5. Conclusions

In this study, multiple tracers were used to label three critical water ages and their corresponding depths under different vegetation conditions on the Loess Plateau. The amounts of new water of transpiration (temporally originating from post-planting precipitation) and old water of transpiration (temporally originating from pre-planting precipitation) were estimated over the vegetation lifespan using the water balance method for two sub-profiles. New water depths in the soil profile were about 5.0 m with a 22-year water age under the apple orchard and 7.4 m with a 17-year water age under the peach orchard, while the maximum water age depths were 26.4 m for the 63-year water age and 19.6 m for the 45-year water age. Deep-rooted vegetation mainly transpired new water, accounting for about 94.97 % of the total transpiration with a transpiration rate of 500.56 mm yr^{-1} under the apple orchard and 97.47 % of the total transpiration with a transpiration rate of 485.52 mm yr^{-1} under the peach orchard. These findings could improve our understanding of hydrological cycle partitioning into different compartments and fluxes in the unsaturated zone from the perspective of water age.

CRediT authorship contribution statement

Guangjie Chen: Data curation, Formal analysis, Investigation, Methodology, Validation, Visualization, Writing – original draft. **Wenjie Wu:** Investigation, Data curation, Methodology, Visualization. **Tingfang Meng:** Investigation, Data curation, Methodology, Visualization. **Mingyi Wen:** Validation, Methodology, Visualization. **Bingcheng Si:** Conceptualization, Funding acquisition, Methodology. **Jianqiang He:** Validation, Methodology, Visualization, Writing – review & editing. **Min Li:** Conceptualization, Funding acquisition, Validation, Methodology, Writing – review & editing. **Qin'ge Dong:** Methodology, Resources, Data curation. **Hao Feng:** Conceptualization, Validation, Methodology, Visualization, Resources, Data curation. **Kadambot H.M. Siddique:** Visualization, Writing – review & editing.

Declaration of Competing Interest

The authors declare that they have no known competing financial interests or personal relationships that could have appeared to influence the work reported in this paper.

Data availability

Data will be made available on request.

Acknowledgments

This work was funded by the National Key R&D Program of China (2021YFD1900700), National Natural Science Foundation of China (41877017; 41630860; 41977064), Fundamental Research Funds for the Central Universities (2452021158), and China 111 project (B12007). We extend our gratitude to Jin Jingjing, the lab manager from the Key Laboratory of Agricultural Soil and Water Engineering in Arid and Semiarid Areas, Ministry of Education, Northwest A&F University.

Appendix A. Supplementary data

Supplementary data to this article can be found online at https://doi.org/10.1016/j.jhydrol.2022.128964.

References

Abbott, B.W., Baranov, V., Mendoza-Lera, C., Nikolakopoulou, M., Harjung, A., Kolbe, T., Balasubramanian, M.N., Vaessen, T.N., Ciocca, F., Campeau, A., Wallin, M.B., Romeijn, P., Antonelli, M., Gonçalves, J., Datry, T., Laverman, A.M., de Dreuzy, J.-R., Hannah, D.M., Krause, S., Oldham, C., Pinay, G., 2016. Using multi-tracer inference to move beyond single-catchment ecohydrology. Earth Sci. Rev. 160, 19–42. https://doi.org/10.1016/j.earscirev.2016.06.014.

Allen, S.T., Kirchner, J.W., Braun, S., Siegwolf, R.T.W., Goldsmith, G.R., 2019. Seasonal origins of soil water used by trees. Hydrol. Earth Syst. Sci. 23 (2), 1199–1210. https://doi.org/10.5194/hess-23-1199-2019.

Allison, G.B., Cook, P.G., Barnett, S.R., Walker, G.R., Jolly, I.D., Hughes, M.W., 1990. Land clearance and river salinisation in the western Murray Basin, Australia. J. Hydrol. 119 (1–4), 1–20. https://doi.org/10.1016/0022-1694(90)90030-2.

Al-Oqaili, F., Good, S.P., Peters, R.T., Finkenbiner, C., Sarwar, A., 2020. Using stable water isotopes to assess the influence of irrigation structural configurations on evaporation losses in semiarid agricultural systems. Agric. For. Meteorol. 291, 108083 https://doi.org/10.1016/j.agrformet.2020.108083.

Armbruster, D.A., Pry, T.A., 2008. Limit of blank, limit of detection and limit of quantitation. Clin. Biochem. Rev. 29, S49–S52.

Barua, S., Cartwright, I., Dresel, P.E., Daly, E., 2021. Using multiple methods to investigate the effects of land-use changes on groundwater recharge in a semi-arid area. Hydrol. Earth Syst. Sci. 25 (1), 89–104. https://doi.org/10.5194/hess-25-89-2021.

Benettin, P., Nehemy, M.F., Asadollahi, M., Pratt, D., Bensimon, M., McDonnell, J.J., Rinaldo, A., 2021. Tracing and closing the water balance in a vegetated lysimeter. Water Resour. Res. 57, e2020. https://doi.org/10.1029/2020wr029049.

Bethke, C.M., Johnson, T.M., 2008. Groundwater age and groundwater age dating. Annu. Rev. Earth Planet. Sci. 36 (1), 121–152. https://doi.org/10.1146/annurev.earth.36.031207.124210.

Beyer, M., Koeniger, P., Gaj, M., Hamutoko, J.T., Wanke, H., Himmelsbach, T., 2016. A deuterium-based labeling technique for the investigation of rooting depths, water uptake dynamics and unsaturated zone water transport in semiarid environments. J. Hydrol. 533, 627–643. https://doi.org/10.1016/j.jhydrol.2015.12.037.

Brinkmann, N., Seeger, S., Weiler, M., Buchmann, N., Eugster, W., Kahmen, A., 2018. Employing stable isotopes to determine the residence times of soil water and the temporal origin of water taken up by Fagus sylvatica and Picea abies in a temperate forest. New Phytol. 219 (4), 1300–1313. https://doi.org/10.1111/nph.15255.

Craig, H., Gordon, L.I., 1965. Deuterium and Oxygen 18 Variation in the Ocean and the Marine Atmosphere. Stable Isotopes in Oceanographic Studies and Paleotemperatures, Spoleto, Italy. Laboratoriodi Geologica Nucleare, Pisa, Italy.

Fan, Y., Miguez-Macho, G., Jobbagy, E.G., Jackson, R.B., Otero-Casal, C., 2017. Hydrologic regulation of plant rooting depth. Proc. Natl. Acad. Sci. U.S.A. 114 (40), 10572–10577. https://doi.org/10.1073/pnas.1712381114.

Foster, S.S.D., 1975. The chalk groundwater tritium anomaly – a possible explanation. J. Hydrol. 25 (1), 159–165. https://doi.org/10.1016/0022-1694(75)90045-1.

Gates, J.B., Scanlon, B.R., Mu, X., Zhang, L., 2011. Impacts of soil conservation on groundwater recharge in the semi-arid Loess Plateau, China. Hydrogeol. J. 19 (4), 865–875. https://doi.org/10.1007/s10040-011-0716-3.

Gee, G.W., Bauder, J.W., 1986. Particle-size analysis. In: Klute, A. (Ed.), In Methods for Soil Analysis. Agronomy 9 Part 1, pp. 383–411.

Geng, Q., Ren, Q., Yan, H., Li, L., Zhao, X., Mu, X., Wu, P., Yu, Q., 2020. Target areas for harmonizing the Grain for Green Programme in Chinas Loess Plateau. Land Degrad. Dev. 31, 325–333. https://doi.org/10.1002/ldr.3451.

Gibson, J.J., Birks, S.J., Edwards, T.W.D., 2008. Global prediction of δA and δ2H-δ18O evaporation slopes for lakes and soil water accounting for seasonality. Global Biogeochem. Cycl. 22 (2), GB2031. https://doi.org/10.1029/2007gb002997.

Good, S.P., Noone, D., Bowen, G., 2015. Hydrologic connectivity constrains partitioning of global terrestrial water fluxes. Science 349 (6244), 175–177. https://doi.org/10.1126/science.aaa5931.

Horita, J., Wesolowski, D.J., 1994. Liquid-vapor fractionation of oxygen and hydrogen isotopes of water from the freezing to the critical temperature. Geochim. Cosmochim. Acta 58 (16), 3425–3437. https://doi.org/10.1016/0016-7037(94)90096-5.

Huang, Y., Chang, Q., Li, Z., 2018. Land use change impacts on the amount and quality of recharge water in the loess tablelands of China. Sci. Total Environ. 628–629, 443–452. https://doi.org/10.1016/j.scitotenv.2018.02.076.

Huang, Y., Evaristo, J., Li, Z., 2019. Multiple tracers reveal different groundwater recharge mechanisms in deep loess deposits. Geoderma 353, 204–212. https://doi.org/10.1016/j.geoderma.2019.06.041.

Huang, T., Pang, Z., Yang, S., Yin, L., 2020. Impact of afforestation on atmospheric recharge to groundwater in a semiarid area. J. Geophys. Res.: Atmos. 125 (9), e2019. https://doi.org/10.1029/2019JD032185.

Huang, L., Shao, M.A., 2019. Advances and perspectives on soil water research in China's Loess Plateau. Earth Sci. Rev. 199, 102962 https://doi.org/10.1016/j.earscirev.2019.102962.

Jasechko, S., Sharp, Z.D., Gibson, J.J., Birks, S.J., Yi, Y., Fawcett, P.J., 2013. Terrestrial water fluxes dominated by transpiration. Nature 496 (7445), 347–350. https://doi.org/10.1038/nature11983.

Jia, Y., Li, T., Shao, M.A., Hao, J., Wang, Y., Jia, X., Zeng, C., Fu, X., Liu, B., Gan, M., Zhao, M., Ju, X., 2019. Disentangling the formation and evolvement mechanism of plants-induced dried soil layers on China's Loess Plateau. Agric. For. Meteorol. 269–270, 57–70. https://doi.org/10.1016/j.agrformet.2019.02.011.

Jia, X., Zhao, C., Wang, Y., Zhu, Y., Wei, X., Shao, M.A., 2020. Traditional dry soil layer index method overestimates soil desiccation severity following conversion of cropland into forest and grassland on China's Loess Plateau. Agric. Ecosyst. Environ. 291, 106794 https://doi.org/10.1016/j.agee.2019.106794.

Koeniger, P., Gaj, M., Beyer, M., Himmelsbach, T., 2016. Review on soil water isotope-based groundwater recharge estimations. Hydrol. Process. 30 (16), 2817–2834. https://doi.org/10.1002/hyp.10775.

Kool, D., Agam, N., Lazarovitch, N., Heitman, J.L., Sauer, T.J., Ben-Gal, A., 2014. A review of approaches for evapotranspiration partitioning. Agric. For. Meteorol. 184, 56–70. https://doi.org/10.1016/j.agrformet.2013.09.003.

Li, Z., Chen, X., Liu, W., Si, B., 2017. Determination of groundwater recharge mechanism in the deep loessial unsaturated zone by environmental tracers. Sci. Total Environ. 586 (15), 827–835. https://doi.org/10.1016/j.scitotenv.2017.02.061.

Li, Z., Jasechko, S., Si, B., 2019c. Uncertainties in tritium mass balance models for groundwater recharge estimation. J. Hydrol. 571, 150–158. https://doi.org/10.1016/j.jhydrol.2019.01.030.

Li, C., Qi, J., Wang, S., Yang, L., Yang, W., Zou, S., Zhu, G., Li, W., 2014. A holistic system approach to understanding underground water dynamics in the Loess Tableland: a case study of the Dongzhi Loess Tableland in Northwest China. Water Resour. Manage. 28 (10), 2937–2951. https://doi.org/10.1007/s11269-014-0647-6.

Li, H., Si, B., Li, M., 2018. Rooting depth controls potential groundwater recharge on hillslopes. J. Hydrol. 564, 164–174. https://doi.org/10.1016/j.jhydrol.2018.07.002.

Li, Z., Si, B., 2018. Reconstructed precipitation tritium leads to overestimated groundwater recharge. J. Geophys. Res. Atmos. 123 (17), 9858–9867. https://doi.org/10.1029/2018jd028405.

Li, H., Si, B., Wu, P., McDonnell, J.J., 2019b. Water mining from the deep critical zone by apple trees growing on loess. Hydrol. Process. 33 (2), 320–327. https://doi.org/10.1002/hyp.13346.

Li, B., Wang, Y., Hill, R., Li, Z., 2019a. Effects of apple orchards converted from farmlands on soil water balance in the deep loess deposits based on HYDRUS-1D model. Agric. Ecosyst. Environ. 285, 106645 https://doi.org/10.1016/j.agee.2019.106645.

Liang, X., Xin, Z., Shen, H., Yan, T., 2022. Deep soil water deficit causes Populus simonii Carr degradation in the Three North Shelterbelt Region of China. J. Hydrol. 612, 128201 https://doi.org/10.1016/j.jhydrol.2022.128201.

Lin, R., Wei, K., 2006. Tritium profiles of pore water in the Chinese loess unsaturated zone: implications for estimation of groundwater recharge. J. Hydrol. 328 (1–2), 192–199. https://doi.org/10.1016/j.jhydrol.2005.12.010.

Liu, J., Song, X., Yuan, G., Sun, X., Yang, L., 2014. Stable isotopic compositions of precipitation in China. Tellus B: Chem. Phys. Meteorol. 66 (1), 22567. https://doi.org/10.3402/tellusb.v66.22567.

Lu, Y., Li, H., Si, B., Li, M., 2020. Chloride tracer of the loess unsaturated zone under sub-humid region: a potential proxy recording high-resolution hydroclimate. Sci. Total Environ. 700, 134465 https://doi.org/10.1016/j.scitotenv.2019.134465.

Markewitz, D., Devine, S., Davidson, E.A., Brando, P., Nepstad, D.C., 2010. Soil moisture depletion under simulated drought in the Amazon: impacts on deep root uptake. New Phytol. 187 (3), 592–607. https://doi.org/10.1111/j.1469-8137.2010.03391.x.

Rossman, N.R., Zlotnik, V.A., Rowe, C.M., Szilagyi, J., 2014. Vadose zone lag time and potential 21st century climate change effects on spatially distributed groundwater recharge in the semi-arid Nebraska Sand Hills. J. Hydrol. 519, 656–669. https://doi.org/10.1016/j.jhydrol.2014.07.057.

Schenk, H.J., Jackson, R.B., 2005. Mapping the global distribution of deep roots in relation to climate and soil characteristics. Geoderma 126 (1–2), 129–140. https://doi.org/10.1016/j.geoderma.2004.11.018.

Schlesinger, W.H., Jasechko, S., 2014. Transpiration in the global water cycle. Agric. For. Meteorol. 189, 115–117. https://doi.org/10.1016/j.agrformet.2014.01.011.

Shao, R., Zhang, B., He, X., Li, Y., Biao, L., Wang, X., Yang, W., He, C., 2021. Historical water storage changes over China's Loess Plateau. Water Resour. Res. 57 (3), e2020. https://doi.org/10.1029/2020WR028661.

Si, B., Jong, E., 2007. Determining long-term (decadal) deep drainage rate using multiple tracers. J. Environ. Qual. 36, 1686–1694. https://doi.org/10.2134/jeq2007.0029.

Skrzypek, G., Mydłowski, A., Dogramaci, S., Hedley, P., Gibson, J.J., Grierson, P.F., 2015. Estimation of evaporative loss based on the stable isotope composition of water using Hydrocalculator. J. Hydrol. 523, 781–789. https://doi.org/10.1016/j.jhydrol.2015.02.010.

Sprenger, M., Tetzlaff, D., Buttle, J., Laudon, H., Soulsby, C., 2018. Water ages in the critical zone of long-term experimental sites in northern latitudes. Hydrol. Earth Syst. Sci. 22 (7), 3965–3981. https://doi.org/10.5194/hess-22-3965-2018.

Sprenger, M., Stumpp, C., Weiler, M., Aeschbach, W., Allen, S.T., Benettin, P., Dubbert, M., Hartmann, A., Hrachowitz, M., Kirchner, J.W., McDonnell, J.J., Orlowski, N., Penna, D., Pfahl, S., Rinderer, M., Rodriguez, N., Schmidt, M., Werner, C., 2019. The demographics of water: a review of water ages in the critical zone. Rev. Geophys. 57 (3), 800–834. https://doi.org/10.1029/2018rg000633.

Suo, L., Huang, M., Zhang, Y., Duan, L., Shan, Y., 2018. Soil moisture dynamics and dominant controls at different spatial scales over semiarid and semi-humid areas. J. Hydrol. 562, 635–647. https://doi.org/10.1016/j.jhydrol.2018.05.036.

Tao, Z., Li, H., Neil, E., Si, B., 2021. Groundwater recharge in hillslopes on the Chinese Loess Plateau. J. Hydrol.: Reg. Stud. 36, 100840 https://doi.org/10.1016/j.ejrh.2021.100840.

Turkeltaub, T., Jia, X., Zhu, Y., Shao, M.A., Binley, A., 2018. Recharge and nitrate transport through the deep vadose zone of the Loess Plateau: a regional-scale model investigation. Water Resour. Res. 54 (7), 4332–4346. https://doi.org/10.1029/2017wr022190.

Wang, Y., Shao, M.A., Zhu, Y., Liu, Z., 2011. Impacts of land use and plant characteristics on dried soil layers in different climatic regions on the Loess Plateau of China. Agric. For. Meteorol. 151 (4), 437–448. https://doi.org/10.1016/j.agrformet.2010.11.016.

Wu, W., Li, H., Feng, H., Si, B., Chen, G., Meng, T., Li, Y., Siddique, K.H.M., 2021. Precipitation dominates the transpiration of both the economic forest (Malus pumila) and ecological forest (Robinia pseudoacacia) on the Loess Plateau after about 15 years of water depletion in deep soil. Agric. For. Meteorol. 297, 108244 https://doi.org/10.1016/j.agrformet.2020.108244.

Wu, W., Tao, Z., Chen, G., Meng, T., Li, Y., Feng, H., Si, B., Manevski, K., Andersen, M.N., Siddique, K.H.M., 2022. Phenology determines water use strategies of three economic tree species in the semi-arid Loess Plateau of China. Agric. For. Meteorol. 312, 108716 https://doi.org/10.1016/j.agrformet.2021.108716.

Xiang, W., Si, B.C., Biswas, A., Li, Z., 2019. Quantifying dual recharge mechanisms in deep unsaturated zone of Chinese Loess Plateau using stable isotopes. Geoderma 337, 773–781. https://doi.org/10.1016/j.geoderma.2018.10.006.

Xiang, W., Si, B., Li, M., Li, H., Lu, Y., Zhao, M., Feng, H., 2021. Stable isotopes of deep soil water retain long-term evaporation loss on China's Loess Plateau. Sci. Total Environ. 784, 147153 https://doi.org/10.1016/j.scitotenv.2021.147153.

Yang, Y., Fu, B.-J., 2017. Soil water migration in the unsaturated zone of semiarid region in China from isotope evidence. Hydrol. Earth Syst. Sci. 21, 1757–1767. https://doi.org/10.5194/hess-21-1757-2017.

Yang, M., Gao, X., Zhao, X., Wang, S., 2022. Quantifying the importance of deep root water uptake for apple trees' hydrological and physiological performance in drylands. J. Hydrol. 606, 127471 https://doi.org/10.1016/j.jhydrol.2022.127471.

Zhang, Z.Q., Evaristo, J., Li, Z., Si, B.C., McDonnell, J.J., 2017. Tritium analysis shows apple trees may be transpiring water several decades old. Hydrol. Process. 31 (5), 1196–1201. https://doi.org/10.1002/hyp.11108.

Zhang, Z., Li, M., Si, B., Feng, H., 2018. Deep rooted apple trees decrease groundwater recharge in the highland region of the Loess Plateau, China. Sci. Total Environ. 622–623, 584–593. https://doi.org/10.1016/j.scitotenv.2017.11.230.

Zhang, Z., Si, B., Li, M., Li, H., 2020. Deficit and recovery of deep soil water following a full cycle of afforestation and deforestation of apple trees on the Loess Plateau, China. Water 12 (4), 989. https://doi.org/10.3390/w12040989.

Zhu, Y.J., Jia, X.X., Shao, M.A., 2018. Loess thickness variations across the Loess Plateau of China. Surv. Geophys. 39 (4), 715–727. https://doi.org/10.1007/s10712-018-9462-6.